

https://dspace.org/

Inhibition of the Complement Pathway Induces Cellular Proliferation and Migration in Pantreatic Ductal Adenocarcinoma

Zanele Nsingwane; P Naicker; Jones Omoshoro-Jones; John Devar; Martin Smith ...

BIOLIFE SAS
https://hdl.handle.net/10539/43330
WOS

Downloaded from a DSpace repository. https://dspace.org/

Article

J. Biol. Regul. Homeost. Agents. 2024; 38(2): 1181–1192
https://doi.org/10.23812/j.biol.regul.homeost.agents.20243802.94

Inhibition of the Complement Pathway Induces Cellular Proliferation and Migration in Pancreatic Ductal Adenocarcinoma

Zanele Nsingwane[1], Previn Naicker[2], Jones Omoshoro-Jones[1,3], John Devar[1,3], Martin Smith[1,3], Geoffrey Candy[1], Tanya Nadine Augustine[4], Ekene Emmanuel Nweke[1,5,*]

[1]Department of Surgery, Faculty of Health Sciences, University of the Witwatersrand, 2193 Johannesburg, South Africa
[2]Future Production Chemicals, Council for Scientific and Industrial Research, 0184 Pretoria, South Africa
[3]Hepatopancreatobiliary (HPB) Surgery Unit, Chris Hani Baragwanath Academic Hospital, 1864 Johannesburg, South Africa
[4]School of Anatomical Sciences, Faculty of Health Sciences, University of the Witwatersrand, 2193 Johannesburg, South Africa
[5]Department of Life and Consumer Sciences, College of Agriculture and Environmental Sciences, University of South Africa, Florida, 1709 Roodepoort, South Africa
*Correspondence: ekene.nweke@wits.ac.za (Ekene Emmanuel Nweke)
Published: 1 February 2024

Background: Pancreatic ductal adenocarcinoma (PDAC) is a lethal cancer with a growing incidence and mortality despite novel therapeutic strategies. Its aggressiveness and difficulty in treatment suggest the need for a better understanding of associated molecular mechanisms that could be targeted for treatment. The complement signalling pathway may play diverse roles in PDAC by eliciting an immune response, inducing inflammatory responses, and elevating pathways linked to chemoresistance. However, their role in the progression of PDAC is not fully understood. This study aimed to identify potential immune response-related targets in a group of patients.

Methods: Thirty tissue samples (tumours and corresponding normal tissues) were obtained from 15 PDAC patients, 34 plasma samples from 25 PDAC patients, six patients with chronic pancreatitis, and three healthy control participants. Targeted pathway-specific polymerase chain reaction (PCR) analysis was conducted to determine the gene expression profiles of immune-response-related genes. The circulating levels of complement proteins C3 and C5 were further investigated. Pharmacological inhibition of the complement pathway in MIA PaCa-2 pancreatic cancer cell lines was performed, and the effect was assessed by cell proliferation, cell migration, and cell cycle assays. Finally, Sequential Window Acquisition of All Theoretical Mass Spectra (SWATH-MS) was performed to identify potential molecular mechanisms during inhibition.

Results: The results identified C3 as overly expressed in early PDAC compared to later stages in plasma ($p = 0.047$). Pharmacological inhibition of the complement pathway led to increased cell growth ($p < 0.0001$), proliferation ($p = 0.001$) and migration ($p = 0.002$) *in vitro*. Proteomic analysis implicated several proteins, such as the mitochondrial and histone proteins, that could play a role in inducing this phenotype.

Conclusion: Complement C3 and C5 are elevated in PDAC samples compared to healthy ones. Furthermore, the inhibition of the complement pathway was shown *in vitro* to result in a more aggressive phenotype by stimulating cellular growth, proliferation, and migration, indicating the involvement of complement C3 and C5 in tumour progression. This study helps to delineate further the role of the complement pathway in PDAC progression.

Keywords: PDAC progression; pancreatic cancer; immune response; complement pathway; complement inhibition; inflammation; proteomics analysis

Introduction

Pancreatic ductal adenocarcinoma (PDAC) is a lethal cancer with a growing incidence and proves difficult to treat [1]. It is widely regarded as non-immunogenic due to its immunosuppressive tumour microenvironment [2]. PDAC lacks distinct symptoms and is typically diagnosed at an advanced stage when resection is impossible. This emphasises the need for early biomarker identification and effective treatment strategies. Recent advances in cancer immunotherapy have ensured some success in numerous cancers, such as melanoma and some lymphomas, but have not yielded improved results in PDAC. Consequently, the five-year survival of PDAC is 12% [3]. Pancreatic cancer is known to be associated with inflammation, and the immune response plays a crucial role in the development and progression of the disease [4]. Inflammatory signals can promote the growth and spread of cancer cells by creating an environment that supports tumour progression [5]. Under-

Copyright: © 2024 The Author(s). Published by Biolife Sas. This is an open access article under the CC BY 4.0 license.
Note: *J. Biol. Regul. Homeost. Agents.* stays neutral with regard to jurisdictional claims in published maps and institutional affiliations.

Please note that certain pages of this article have been removed in order to reduce the file size so that the PDF can be uploaded on the system (the system has a limit of 1MB for files and several PDF files are larger than this).

The first and last pages of each paper (with full bibliographic details and affiliations) are included.

If the entire unredacted paper is required, this can be emailed directly to whomever requires them by contacting Dr. Busisiwe Maseko on Busisiwe.Maseko@wits.ac.za

Journal of
BIOLOGICAL REGULATORS
and Homeostatic Agents

standing the interplay between inflammation and immune response in pancreatic cancer is essential for developing effective therapeutic strategies.

The complement signalling pathway, which involves the activation of specific complement proteins, plays a vital role in immune surveillance and facilitates the elimination of invading pathogens and 'non-self' antigens [6]. Once activated, these complement proteins can trigger a cascade of events that ultimately destroy foreign substances. Aberrations in this pathway are associated with chronic inflammation, cancer, and autoimmune diseases [7]. This pathway can be activated via three main routes: classical, mannose-binding lectin and alternative pathways, all of which have the complement C3 as a central protein. C3 functions as a master switch that regulates all downstream factors and proteins, including the complement C5, responsible for pathogen elimination via the membrane attack complex (MAC). Understanding the complement system's role in cancer has evolved over the years, with complement proteins now implicated in several hallmarks of cancer [8,9]. Although the complement pathway is involved in eliciting immune response, it may also play a tumour-promoting role [10]. Activating the complement pathway can lead to heightened inflammation, creating a conducive environment that promotes the growth and spread of cancer cells [11]. In PDAC, increased complement protein levels have been demonstrated to elevate anaphylatoxins, C3a and C5a, which directly induce Tumour Necrosis Factor-alpha (TNF-α) and Interleukin-1β (IL-1β) [6]. Furthermore, C3 and C5 are linked to chemoresistance by potential interactions with several pathways such as nuclear factor kappa B (NF-κB), phosphoinositide-3-kinase/protein kinase B (PI3K/AKT), C-mesenchymal-epithelial transition factor (C-MET) and the signal transducer and activator of transcription 3 (STAT3) pathways [6,12]. However, the mechanisms underpinning these interactions are not fully understood.

This study aimed to identify potential immune response-related targets associated with PDAC in a cohort of patients of African ancestry. Tumour and plasma samples from PDAC patients were profiled using immune-response pathway-specific polymerase chain reaction (PCR) arrays, real-time PCR and Enzyme-linked immunosorbent assay (ELISA). The levels of complement proteins C3 and C5 were confirmed to vary with tumour severity. A pancreatic cancer cell line model (MIA PaCa-2) was used to demonstrate the effects of the pharmacological inhibition of the complement pathway. Additionally, Sequential Window Acquisition of All Theoretical Mass Spectra (SWATH-MS) was conducted to identify proteins that were dysregulated following inhibition of the complement pathway.

Materials and Methods

Patient Selection and Recruitment

Patients were recruited from the hepatopancreatobiliary (HPB) unit of Chris Hani Baragwanath Academic Hospital (CHBAH) in Johannesburg, South Africa, between January 2017 and March 2020. The inclusion criteria encompassed individuals of African ancestry aged 18 years and above who were clinically and histologically diagnosed with PDAC. Patients presenting with acute inflammation, sepsis, organ failure and those undergoing therapy were excluded from the study. A total of 49 participants were recruited and included in this study. This research was conducted in accordance with the Declaration of Helsinki. All PDAC patients were clinically and histopathologically diagnosed with pancreatic ductal adenocarcinoma (PDAC) following abdominal screening using a contrast-enhanced triple-phased CT scan. Histopathological diagnosis was either endoscopic or surgical. Endoscopic pathological diagnosis was by brush cytopathology of structures at endoscopic retrograde cholangiopancreatography (ERCP) or biopsy of pancreas mass by endoscopic ultrasonography (EUS). All participants signed an informed consent form, and ethical clearance for using human specimens was obtained from the University of the Witwatersrand Human Research Ethics Committee (Medical) (M190734 and M140317).

Tissues: Biopsy samples (a tumour and corresponding normal tissue) from 15 patients [13] scheduled for a Whipple procedure (surgical resection of cancerous tumours located on the head of the pancreas), were immediately immersed in RNA later™ stabilisation solution (2857138, Invitrogen™, Waltham, MA, USA).

Plasma: A separate cohort of 25 PDAC patients (13 resectable, eight locally advanced and four metastatic) was categorised according to the National Comprehensive Cancer Network guidelines (NCCN) [14]. Six chronic pancreatitis (an inflammatory disease affecting the pancreas) patients were recruited to act as a control group as it has been identified as a risk factor for pancreatic cancer [15]. Individuals (three) who self-reported being in good health and not taking any medication were recruited as healthy control participants. Whole blood (10 mL) was collected into Ethylenediaminetetraacetic acid (EDTA) vacutainer tubes (368861, BD Biosciences, Franklin Lakes, NJ, USA) by venepuncture and processed within 2 h of collection. The blood was separated by gravity and then centrifuged at 3000 g at 4 ºC for 30 minutes, and the isolated plasma was aliquoted (500 µL) into Eppendorf tubes. All samples were stored in a freezer at –80 °C until required, and analysis was conducted within six months.

Total RNA Extraction from Tissues and Cells

Total RNA was extracted using the TRIzol method [16]. Tissues (15–25 mg) were shredded into small pieces

using sterilised surgical blades and transferred into 15 mL Falcon tubes containing 700 µL of TRIzol reagent (T9424, Sigma Aldrich, St Louis, MO, USA) and then homogenised using a TissueRuptor (9002755, Qiagen, Hilden, Germany). For the MIA PaCa-2 cells, a cell pellet was resuspended in 700 µL of TRIzol homogenous mixture, transferred into 1.5 mL Eppendorf tubes and allowed to stand for five minutes at room temperature to ensure nucleoprotein complexes were fully dissociated. Chloroform (150 µL) (02487, Sigma Aldrich, St Louis, MO, USA) was added and shaken vigorously for 15 seconds until the mixture turned milky, then left to stand for eight minutes before being centrifuged at 12,000 g for 10 minutes at 4 ºC. The aqueous phase was transferred into sterile Eppendorf tubes, and 350 µL of isopropanol (I9516, Sigma Aldrich, St Louis, MO, USA) was added to the sample, mixed by resuspension, and allowed to stand for seven minutes. The mixture was centrifuged at 12,000 g for eight minutes at 4 ºC. The supernatant was discarded, and the pellet was washed with 700 µL of 75% cold ethanol (E7148, Sigma Aldrich, St Louis, MO, USA). The sample was vortexed for five seconds and centrifuged at 7500 g for five minutes at 4 ºC. The supernatant was discarded, and the pellet was air-dried for 10 minutes and placed into a dry bath (55 ºC) for further drying. Nuclease-free water (30 µL) (3098, Sigma Aldrich, St Louis, MO, USA) was added to the pellet, mixed repeatedly with a pipette, placed in the heating block for five minutes at 55 ºC, and immediately placed on ice. Total RNA concentration and quality were assessed using the Nanodrop™ 2000 (ND2000CLAPTOP, ThermoFisher Scientific, Waltham, MA, USA). The A260/A280 and A260/230 measurements of the samples were all above 2.0.

Pathway-Focused PCR Array Analysis

The RT^2 First Strand kit (330401, Qiagen, Hilden, Germany) was used for cDNA synthesis from two micrograms of total RNA per the manufacturer's instructions. The RT^2 Profiler PCR Human Innate and Adaptive Immune Responses panel (PAHS-052ZA 330231, Qiagen, Hilden, Germany) were used to perform a pathway-focused gene expression analysis of immune response genes. The PCR mix was prepared per the manufacturer's instructions and run on the QuantStudio1 real-time thermocycler (A40427, ThermoFisher Scientific, Waltham, MA, USA). The Ct values were exported, and Fold changes were analysed using the QIAGEN RT^2 Profiler PCR analysis software tool (https://www.qiagen.com/us/product-categories/instruments-and-automation/analytics-software accessed 12 September 2019).

Verification of Gene Targets Using Real-Time PCR

Verification of gene targets on the tissue samples was achieved by performing cDNA synthesis followed by real-time PCR according to the MIQE guidelines [17]. The Invitrogen™ SuperScript™ VILO™ cDNA synthesis kit (11754050, ThermoFisher Scientific, Waltham, MA, USA) was used, followed by real-time PCR. Validated predesigned TaqMan Gene Expression assays were used for the three genes: *C3* (Assay ID-Hs00163811_m1, 4331182, ThermoFisher Scientific, Waltham, MA, USA), *C5* (Assay ID-Hs01004342_m1, 4331182, ThermoFisher Scientific, Waltham, MA, USA) and mitochondrial ribosomal protein L19 (*MRPL19*) (Assay ID-Hs00608519_m1, ThermoFisher Scientific, Waltham, MA, USA). The method involved adding 5 µL of TaqMan® Gene Expression Master Mix (2X) (4369016, ThermoFisher Scientific, Waltham, MA, USA), 0.5 µL TaqMan® Gene Expression Assay 20X for target gene and reference gene, 3 µL of cDNA template, Human Male Raji cDNA template (controls), and 1 µL nuclease-free water to a PCR plate, briefly vortexed, centrifuged and run according to the manufacturer's instructions. The targets were *C3* and *C5,* with *MRPL-19* as a reference gene. Fold changes were determined using the $2^{-\Delta\Delta Ct}$ method [18].

Enzyme-Linked Immunosorbent Assay (ELISA) Analysis

The human complement C3 and C5 ELISA kits (ab108822 and ab125963, Abcam, Cambridge, UK) were used to quantitatively measure plasma C3 and C5 across PDAC patients in different stages (resectable, locally advanced and metastatic), chronic pancreatitis patients and healthy individuals. Based on the manufacturer's recommendation, plasma samples were diluted 1:800 into 1X diluent M for C3 and 1:20,000 into 1X diluent N for C5. 1X wash buffer, 1X Streptavidin-Peroxidase conjugate, 1X biotinylated complement C3/C5, seven standards and a blank were prepared according to the manufacturer's protocol. Twenty-five microlitres and 50 mL of samples and standards were added to each well of a pre-coated and blocked 96-well microtiter plate for C3 and C5. For C3, 25 µL of 1X biotinylated complement C3 antibody was added and incubated at RT for 2 h. For C5, 50 µL of 1X biotinylated complement C5 antibody was incubated for 1 h. Plates were washed per manufacturer guidelines, followed by adding 50 µL 1X Streptavidin-Peroxidase conjugate to all wells for 30 minutes at RT. Stop solution (50 µL) was added to each well, and the colour change from blue to yellow and absorbance were measured at 450 nm immediately using the Biochrom Anthos 2010 Microplate reader (GF1755011, Biochrom Ltd, Cambridge Camb, UK).

Cell Culture and Treatment

The pancreatic cancer cell line MIA PaCa-2, representing a pancreatic cancer model, was used in this study. The cell line was obtained from the Japanese Cancer Research Resources Bank (JRCB) cell bank (Cat no JCRB0070) with the appropriate and extensive details confirming that they were MIA PaCa-2 cells, including DNA profile (STR) (https://cellbank.nibiohn.go.jp/~{}cel

Journal of
BIOLOGICAL REGULATORS
and Homeostatic Agents

lbank/en/search_res_det.cgi?ID=245). MIA PaCa-2 cells were derived from a 65-year-old Caucasian male patient with pancreatic adenocarcinoma located at the head and tail of the pancreas [19]. The MIA PaCa-2 were grown in Dulbecco's Modified Eagle Medium (DMEM) (D8900, Sigma Aldrich, St Louis, MO, USA) with 10% fetal bovine serum (FBS) (12107C, Sigma Aldrich, St Louis, MO, USA) and 1% penicillin-streptomycin (P4333, Sigma Aldrich, St Louis, MO, USA) and maintained in an incubator at 37 °C in 5% CO_2 and 95% air. Mycoplasma detection was conducted (**Supplementary Fig. 1)** as previously described [20]. Compstatin (2585, Tocris Bioscience, Bristol, UK) was used to inhibit the complement pathway pharmacologically [21], dimethyl sulfoxide (DMSO) (589569, Sigma Aldrich, St Louis, MO, USA) as vehicle control, and gemcitabine (Y0000675-50 mg, Sigma Aldrich, St Louis, MO, USA) was used as a positive control. Viable cell counts were determined using the trypan blue exclusion assay by adding 10 µL cells to trypan blue (1:1 ratio) to the cell suspension and counting on a TC20TM automated cell counter (1450102, Bio-Rad Laboratories, Hercules, CA, USA).

Cell Proliferation Assay Using Methoxynitrosulfophenyl-Tetrazolium Carboxanilide (XTT)

The cell proliferation kit II (XTT) (11465015001, Sigma Aldrich, St Louis, MO, USA) colourimetric assay was employed to quantify cell proliferation, viability, and cytotoxicity in pancreatic cancer MIA PaCa-2 cells. Cells were cultured, and viability was determined as described above. Viable MIA PaCa-2 cells (2.5×10^3, 5×10^4 and 1×10^5 cells/well) were seeded in different 96-well plates (8404, ThermoFisher Scientific, Waltham, MA, USA) in 200µl complete medium in triplicate and incubated at 37 °C, 5% CO_2 for 24 h. Once cells reached 60–70% confluence, they were treated with a range (0–100 µM) of complement inhibitor (Compstatin), a dose-response curve was used to determine the effective dose and real-time PCR was conducted on treated cells with the effective dose concentration to confirm inhibition. Controls included a negative control (normal DMEM + 10% FBS + 1% penstrep and cells), the vehicle control (0.1% DMSO in complete medium), cells treated with gemcitabine as a positive control and medium with no cells as a blank) for 24 and 48 h. Absorbance was measured on a spectrophotometer (MULTISKAN Sky, A51119500C, ThermoFisher Scientific, Waltham, MA, USA) at 450 nm with a reference wavelength of 690 nm. Percentage survival for each sample was calculated as $100 \times [(OD_{450}$ of sample – OD_{450} of negative control) / (OD_{450} of positive control – OD_{450} of negative control)].

Cell Cycle Analysis

Measurements of the percentage of cells in the G0/G1, S and G2/M phases of the cell cycle were based on analysing DNA content using the single parameter-based propidium iodide staining technique (556463, BD Biosciences, Franklin Lakes, NJ, USA). MIA Paca-2 cells were counted, 2×10^6 viable cells were seeded in duplicate and left to grow for 24 h. Cells were treated with 6 µM Compstatin to inhibit the complement pathway and with 0.1% DMSO as vehicle control. Following trypsinisation, cells were centrifuged at 250 ×g for five minutes, fixed in cold 70% ethanol, and stored at –20 °C for at least 24 h. For permeabilisation and removal of RNA, 500 µL of 2 mg/mL RNAse A in 0.1% Triton X-100 in Phosphate Buffered Saline (PBS) (223142, BD Biosciences, Franklin Lakes, NJ, USA) and 400 µL of 500 µg/mL propidium iodide dye solution in PBS was resuspended with 100 µL of the sample. The suspension was incubated at room temperature for 30 minutes, and fluorescence was measured using the BD LSR Fortessa™ Analyser and FACS Diva software (v9, BD Biosciences, Franklin Lakes, NJ, USA). The cell cycle phase was estimated using FlowJo™ software (v10, BD Biosciences, Franklin Lakes, NJ, USA).

Cell Migration (Scratch Assay)

Viable MIA PaCa-2 cells (1×10^5), counted as previously mentioned, were seeded in a 24-well plate (142475, ThermoFisher Scientific, Waltham, MA, USA) by adding 1×10^5 µL cell and media solution to each well in duplicate. Plates were incubated at 37 °C, 5% CO_2, for 24 h. Once cells reached 80–100% confluence, the cell monolayer was imaged using the Olympus iX51 phase contrast microscope (iX51, Wirsam Scientific & Precision Equipment Ltd, Johannesburg, South Africa), followed by washing cells twice with 0.1 M PBS. A scratch wound was made across the wells on the second wash using a sterile 10 µL pipette tip. The cells were then washed three times with PBS. Cells were exposed to a low serum medium supplemented with 1% FBS instead of the standard 10% FBS [16,22] to reduce nutrient levels, allowing the cells to prioritise migration over proliferation (albeit with some residual proliferation activity) to redirect cellular focus from proliferation to migration while maintaining viability. Cells were treated with 6 µM Compstatin to inhibit complement activation; 0.1% DMSO was used as vehicle control. Images of the scratched area were captured using the Olympus iX51 phase contrast microscope with CellSens Software (v3.2, Olympus, Tokyo, Japan) at 0 h, 6 h, 12 h and 24 h. Image J software (v2.9.0, National Institute of Health, Bethesda, MD, USA) was used to measure the distance between the scratched cells [23]. The following calculation was used to measure the rate of cell migration (Dinitial – Dfinal) × 100 / Dinitial, where D is distance.

Proteomic Analysis Using SWATH-MS Spectrometry

MIA PaCa-2 cells were counted, and 1×10^5 viable cells were seeded in duplicate in a 24-well plate and left to grow for 24 h before being treated with 6 µM Comp-

statin to inhibit the complement pathway by targeting C3. A cell pellet was prepared by washing adherent cells with PBS and adding trypsin-EDTA to detach the cells. Cells were centrifuged at 250 ×g for five minutes. The pellet was washed at least four times with PBS, and a dry pellet was stored at –80 ºC until processing. Treated and untreated cell pellets were resuspended in 50 mM Tris-HCl pH 8.0, containing 2% SDS. The protein concentration was measured using the Pierce Bicinchoninic assay (23225, ThermoFisher Scientific, Waltham, MA, USA), per the manufacturer's instruction. Protein samples (10 µg per sample) were reduced with 5 mM tris (2-carboxyethyl) phosphine and alkylated with 10 mM 2-chloroacetamide at room temperature for 20 minutes. Samples were purified of detergents and salts using MagReSyn™ HILIC beads (MR-HLC005, ReSyn Biosciences Robindale, Randburg, South Africa) as previously described [13,24]. On-bead protein digestion was performed using a 1:20 and 1:100 protease:protein ratio for sequencing-grade trypsin and Lys-C, respectively. The resultant peptides were dried and stored at –80 °C before Liquid chromatography-mass spectrometry (LC-MS). Approximately 1 µg of peptides per sample was analysed using a Dionex Ultimate 3000 RSLC system coupled to a Sciex 5600 TripleTOF mass spectrometer. Injected peptides were de-salted inline using an Acclaim PepMap C18 trap column (75 µM × 2 cm: 2 min at 5 $\mu L.min^{-1}$ using 2% Acetonitrile (can)/0.2% Formic (FA)). Trapped peptides were gradient eluted and separated on a Waters Acquity CSH C18 NanoEase column (75 µM × 25 cm, 1.7 µm particle size) at a flow rate of 0.3 $\mu L.min^{-1}$ with a gradient of 6–40% B over 90 minutes (A: 0.1% FA; B: 80% ACN/0.1% FA). For sequential window Sequential Window Acquisition of All Theoretical (SWATH), precursor scans were acquired from 400–1100 m/z with 50 msec accumulation time. Fragment ions were acquired from 200–1800 m/z for 48 variable-width precursor windows with 0.5 Da overlap between windows and 20 milliseconds accumulation time per window. SWATH data was processed using Spectronaut software v17 (Biognosys, Schlieren, Switzerland). The default direct DIA identification and quantification settings were used for data processing. Carbamidomethylation was added as a fixed modification, and N-terminal acetylation and methionine oxidation were added as variable modifications. Swiss-Prot human sequences (downloaded on 03 March 2023 from www.uniprot.org) and common contaminating proteins were used as the search database. A q-value ≤0.01 cut-off was applied at the precursor and protein levels. Quantification was performed at the MS1 and MS2 levels. Label-free cross-run normalisation was employed using a global normalisation strategy. Candidate dysregulated proteins were filtered at a q-value ≤0.01 and absolute Log2 Fold change (FC) ≥0.58.

Statistical and Bioinformatics Analyses

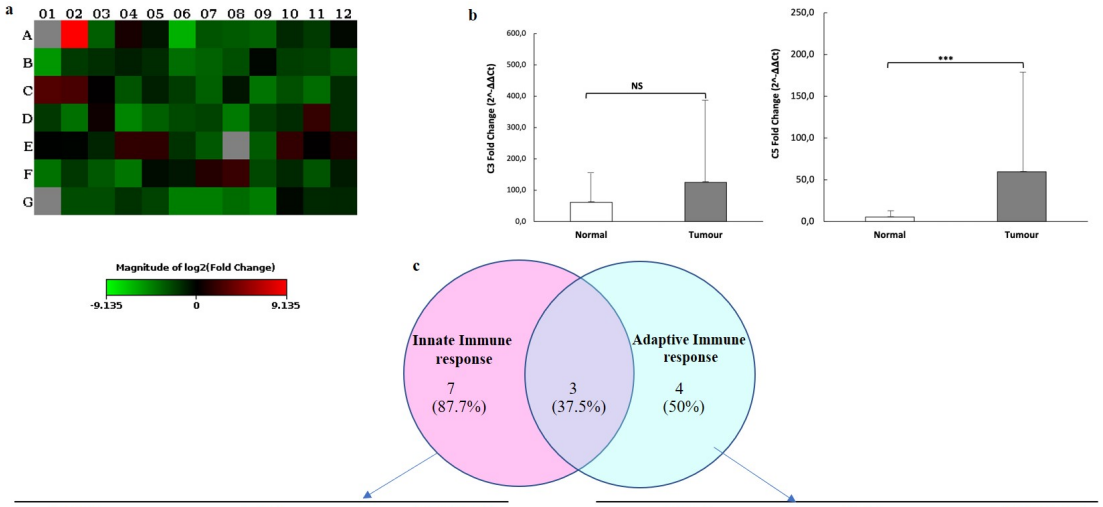
For the ELISA analysis, the Kruskal-Wallis and median tests were used to compare differences between groups due to a small sample size, and the Mann-Whitney U test was performed for post hoc analysis. A one-way Analysis of variance (ANOVA) was used for the real-time analysis to compare the tumour and normal samples. A one-way ANOVA and a Tukey post hoc test were used for cell-based analysis. Spearman correlation analyses were also conducted, and the differences were regarded as significant at $p < 0.05$ for all tests. Functional enrichment analyses were performed on all the dysregulated proteins. Interaction network analysis and visualisation were performed using Cytoscape v3.8.2 [25]. The StringApp v2.0.1 [26] and Reactome v8.0.5 [27] plugins on Cytoscape were used to determine the molecular functions, cell compartments and pathways enriched by the dysregulated proteins. The proteins were queried with filters including *Homo sapiens* as the reference species, a confidence cut-off score of 0.4 and zero additional interactors. Single non-interacting proteins were excluded from the interaction network.

Results

Dysregulated Immune Response Genes in Pancreatic Tumours

The gene expression profile of immune response genes was investigated in pancreatic tumours compared to corresponding normal tissues. Altogether, 13 and 62 genes were upregulated and downregulated, respectively (Fig. 1a, **Supplementary Table 1**). *C3* was the most upregulated gene (Fold change = 562.22), and C-C chemokine receptor type 4 (*CCR4*) was the most downregulated gene (Fold change = –83.19). Furthermore, among the top five upregulated targets, three were major histocompatibility complex molecules, and their expression levels were 20–100 times lower than the *C3*. Real-time PCR was employed to validate the expression of the complement *C3* in the sample group as samples were pooled previously for the RT^2 profiler PCR array. Although the increase of the complement *C3* in tumours (125.3 ± 393.79) compared to normal tissue (61.9 ± 162.09) was confirmed, it was not statistically significant ($p = 0.72$). We further evaluated the expression of another crucial downstream component of the complement pathway, *C5*, which was not included in the PCR array. A significant increase in the expression of complement *C5* in tumours (59.8 ± 166.42) compared to normal tissues (5.4 ± 2.58) was observed ($p < 0.0001$) (Fig. 1b). Moreover, on examining the top five upregulated genes; *C3*, β_2 microglobulin (*B2M*), human leukocyte antigen-A (*HLA-A*), ribosomal protein lateral stalk subunit P0 (*RPLP0*), human leukocyte antigen-E (*HLA-E*), and downregulated genes; C-C chemokine receptor type 4 (*CCR4*), CD40 Ligand (*CD40LG*), Interleukin-2 (*IL-2*), Toll-like receptor 7 (*TLR7*), Toll-like receptor 6 (*TLR-6*), it was observed that

Journal of
BIOLOGICAL REGULATORS
and Homeostatic Agents



Pathway	Genes	Number/Total
Innate Immune response	*C3,IL-2,TLR-6, TLR7, HLA-A, HLA-E, CD40LG*	7/8
Humoral Immunity	*C3*	1/8
Inflammatory response	*C3*	1/8
Cytokine	*IL-2*	1/8
Pattern Recognition Receptor	*TLR-6, TLR-7*	2/8
Defense response to bacteria	*TLR-6*	1/8
Defense response to viruses	*HLA-A, TLR-7*	2/8

Pathway	Genes	Number/Total
Adaptive immune response	*CCR4,CD40LG,HLA-A,IL-2*	4/8
Th2 markers and Immune response	*CCR4*	1/8
Treg markers	*CCR4*	1/8

Fig. 1. Gene expression profiles of immune response genes in pancreatic ductal adenocarcinoma (PDAC) tumours. (a) Heatmap showing differentially expressed genes in the form of Fold regulation. Red represents upregulated genes with positive values, and green represents downregulated targets. (b) Real-time polymerase chain reaction (PCR) verifying the gene expression profile of complement *C3* and *C5* in resectable PDAC tumours. *C3* and *C5* are upregulated in pancreatic tumours and downregulated in normal tissues. Values are indicated as mean ± standard deviation (SD). (c) The Venn diagram shows that most genes function predominantly in the innate immune response but also have some roles in the adaptive immune response. NS indicates non-significant, *** indicates $p < 0.0001$. *IL-2*, Interleukin-2; *TLR-6*, Toll-like receptor 6; *TLR7*, Toll-like receptor 7; *HLA-A*, human leukocyte antigen-A; *HLA-E*, human leukocyte antigen-E; *CD40LG*, CD40 Ligand.

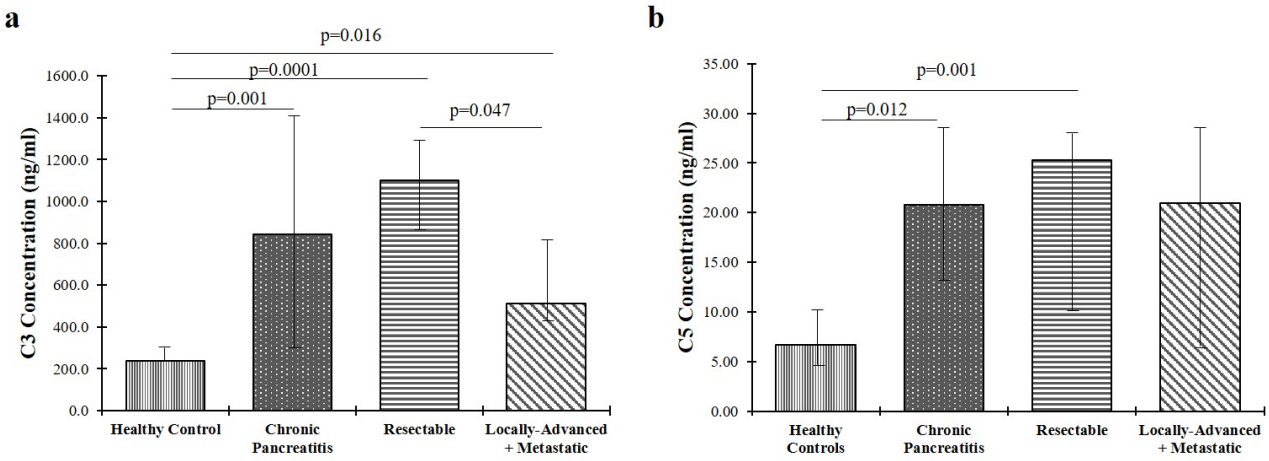


Fig. 2. Protein expression levels of C3 and C5 in plasma of PDAC patients. (a,b) A decreasing trend is observed in all PDAC samples from early- to late-stage disease. Healthy individuals express lower levels of C3 and C5 compared to other groups. The experiment was carried out twice, n = 2. Values are indicated in median [IQR]. IQR, Interquartile range.

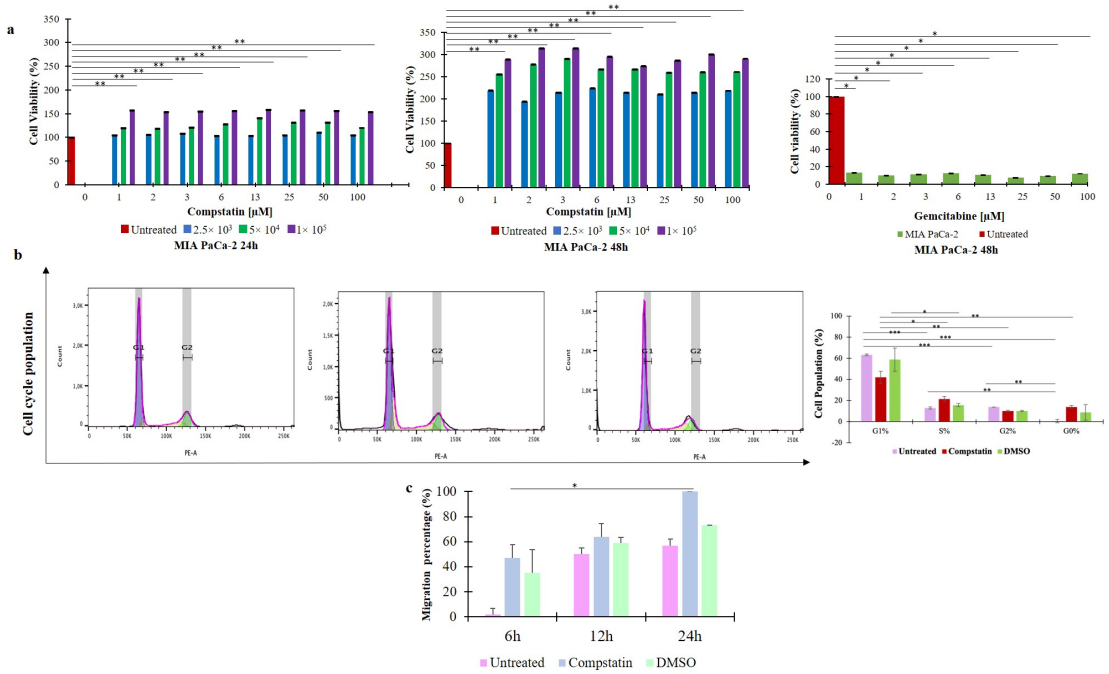


Fig. 3. Enhanced Cell Proliferation and Migration Induced by Complement Inhibition in MIA PaCA-2 cells. (a) Inhibition of the complement pathway induced cell proliferation, as evidenced by increased viability (>100%) in MIA PaCa-2 cells over 48 h, whereas gemcitabine was toxic to MIA PaCa-2. (b) Complement inhibition allowed cells to transition from G1 to S phase, showing increased cell division. (c) Complement inhibition enhances cell migration, compared to untreated and dimethyl sulfoxide (DMSO) vehicle controls. The cell proliferation assay was performed in triplicate (n = 3); the cell cycle and migration assays were performed in duplicate (n = 2). Values are indicated as mean ± SD, $^{*}p < 0.05$, $^{**}p < 0.001$, $^{***}p < 0.0001$, respectively. PE-A, Phycoerythrin dye.

these genes function primarily in the innate immune response but are also involved in part of the adaptive immune response based on their classification in the array panel (Fig. 1c).

Complement C3 and C5 are Elevated in the Plasma of Early-Stage PDAC Patients

The levels of C3 and C5 were investigated in the plasma of a cohort of PDAC patients at different disease stages (**Supplementary Table 2**) and compared to chronic pancreatitis patients and healthy individuals. There were no observed significant changes across the different tumour stages. However, a significant reduction (p = 0.047) in C3 levels was observed when patients with early-stage (resectable) cancer (1099 ± [851–1253] ng/mL) were compared to those with advanced-stage disease (locally advanced and metastatic) (511 ± [430–821] ng/mL) (Fig. 2a). The levels of C5 were increased in all patient groups, including cancer and chronic pancreatitis patients, compared to healthy individuals. Additionally, C5 was shown to be significantly elevated in patients with resectable PDAC (25.3 ± [10.4–26.6] ng/mL) compared to healthy individuals (6.7 ± [4.9–10.5] ng/mL) (p = 0.001) (Fig. 2b). Although there was a reduction in its levels in late-stage disease compared to early-stage, this was not significant. Furthermore, additional statistical analysis demonstrated a positive correlation (r = 0.45669) between complement C5 and the clinical inflammatory marker C-reactive protein (CRP) (p = 0.0098) (**Supplementary Fig. 2**).

Pharmacological Inhibition of the Complement Pathway Induces Cell Proliferation, Cell Division and Migration of MIA PaCa-2 Cells

Cells were treated with Compstatin to investigate the implications of reduced complement pathway activation further, and cell-based analyses were performed. First, the inhibition of the complement pathway was confirmed by reduced C3 and C5 levels (**Supplementary Fig. 3**) after 24 h of treatment with 6 μM Compstatin. The XTT cell proliferation assay showed that complement C3 inhibition resulted in a significant increase (p = 0.001) (Fig. 3a, **Supplementary Table 3**) in the number of viable MIA PaCa-2 cells, indicative of heightened cell proliferation, compared to untreated cells (Fig. 3a). In contrast, treatment with gemcitabine, used as a positive control, reduced cell viability in both normal and cancer cells. Flow cytometry was used to investigate the effect of complement inhibition on the cell cycle of MIA PaCa-2 cells. The findings showed that untreated cells were significantly higher ($p < 0.0001$) in the G1 phase (63.4 ± 6.84%) compared to the G0 phase (0.52 ± 6.84%). However, after Compstatin treatment, the cells

Table 1. Top 10 up- and down-regulated pathways when the complement pathway was pharmacologically inhibited in pancreatic cancer cells.

UPREGULATED			DOWNREGULATED		
Pathway name	*p*-value	Proteins enriched	Pathway name	*p*-value	Proteins enriched
MTF1 activates gene expression	3.95×10^{-6}	CSRP1	RMTs methylate histone arginines	7.96×10^{-10}	H2AC12, H2AC19, H2AJ, H2AC14, H2AC20, H2AC17, H2AC7
Response to metal ions	0.004	CSRP1	Metalloprotease DUBs	3.58×10^{-8}	H2AC12, H2AC19, H2AC14, H2AC20, H2AC17, H2AC7
Mitochondrial translation termination	0.007	MRPL4, MRPL47, MRRF	Packaging of Telomere Ends	1.46×10^{-6}	H2AC12, H2AC19, H2AJ, H2AC14, H2AC20, H2AC7
NFE2L2 regulating antioxidant/detoxification enzymes	0.009	GCLC	HDACs deacetylate histones	1.81×10^{-6}	H2AC12, H2AC19, H2AC14, H2AC20, H2AC17, H2AC7
RNA Polymerase I Transcription Initiation	0.019	EHMT2, POLR1D	DNA methylation	1.95×10^{-6}	H2AC12, H2AC19, H2AJ, H2AC14, H2AC20, H2AC7
Synthesis of very long-chain fatty acyl-CoAs	0.019	ACSL3, HACD3	RHO GTPase Effectors	2.43×10^{-6}	PIK3R4, S100A8, PRKACA, S100A9, RHOC, TUBB4A, H2AC12, H2AC19, H2AJ, H2AC14, H2AC20, H2AC7
Membrane trafficking	0.021	ACBD3, CALM, SCOC, AP4S1, MCFD2, ARF5, RABGAP1	Recognition and association of DNA glycosylase with site containing an affected purine	2.90×10^{-6}	H2AC12, H2AC19, H2AJ, H2AC14, H2AC20, H2AC7
KEAP1-NFE2L2 pathway	0.023	GCLC, PSME1	Regulation of MECP2 expression and activity	3.29×10^{-6}	MECP2
Loss of phosphorylation of MECP2 at T308	0.029	CALM1	Assembly of the ORC complex at the origin of replication	3.29×10^{-6}	H2AC12, H2AC19, H2AJ, H2AC14, H2AC20, H2AC7
RUNX1 regulates transcription of genes involved in BCR signalling	0.029	ELF2	HATs acetylate histones	3.43×10^{-6}	H2AC12, H2AC19, H2AJ, H2AC14, H2AC20, H2AC17, H2AC7,TAF9

MTF1, metal regulatory transcription factor 1; RMTs, arginine methyltransferases; NFE2L2, nuclear factor erythroid 2-like 2; KEAP1, kelch like ECH associated protein 1; MECP2, methyl CpG binding protein 2; RUNX1, Runt-related transcription factor 1; CSRP, Cysteine and Glycine Rich Protein; MRPL, Mitochondrial Ribosomal Protein L; MRRF, Mitochondrial Ribosome Recycling Factor; EHMT2, Euchromatin Histone Methyltransferase II; GCLC, Glutamate Cysteine Ligase catalytic subunit; POLR1D, RNA Polymerase I and III subunit D; ACSL3, acyl-CoA synthetase long chain family member 3; HACD3, 3-hydroxyacyl-CoA dehydratase 3; ACBD3, acyl-CoA binding domain containing 3; CALM, calmodulin; SCOC, short coiled-coil protein; AP4S1, adaptor related protein complex 4 subunit sigma 1; MCFD2, multiple coagulation factor deficiency 2, ER cargo receptor complex subunit; ARF5, ADP ribosylation factor 5; RABGAP1, RAB GTPase activating protein 1; PSME1, proteasome activator subunit 1; ELF2, E74 like ETS transcription factor 2; TAF9, TATA-box binding protein associated factor 9; PIK3R4, phosphoinositide-3-kinase regulatory subunit 4; S100A, S100 calcium binding protein A; PRKACA, protein kinase cAMP-activated catalytic subunit alpha.

Journal of BIOLOGICAL REGULATORS and Homeostatic Agents

exhibited a significant reduction ($p = 0.004$) in the G1 phase (42.0 ± 42.6%) and an increase in the S phase (21.4 ± 42.6%) necessary for DNA replication and repair, and also increased in G0 phase (13.9 ± 42.6%), though the increase was not statistically significant ($p = 0.5055$) (Fig. 3b, **Supplementary Table 4**). The scratch assay showed complement inhibition accelerates cell migration in MIA PaCa-2 cells. A significant increase ($p = 0.002$) in migration was observed from 0 h to 24 h following treatment with Compstatin (Fig. 3c and **Supplementary Fig. 4**).

Proteins Dysregulated with Inhibition of the Complement Pathway

MIA PaCa-2 cells were exposed to Compstatin for 24 h to delineate the potential molecular mechanisms linked with inhibiting the complement pathway in PDAC. Following treatment, SWATH-MS was used to conduct a proteomic analysis, and the results identified a total of 2814 protein groups. A comparison of the Compstatin-treated cells with untreated cells showed 53 upregulated and 60 downregulated proteins (**Supplementary Table 5**). Furthermore, the upregulated proteins included a variety of crucial proteins such as the Cysteine and Glycine Rich Protein (CSRP) 1, Mitochondrial Ribosomal Protein (MRPL4, MRPL47), Mitochondrial Ribosome Recycling Factor (MRRF), Glutamate Cysteine Ligase catalytic subunit (GCLC), Euchromatin Histone Methyltransferase II (EHMT2) and RNA Polymerase I and III subunit D (POLR1D). Moreover, the H2A Clustered Histone family of molecules (H2AJ, H2AC7, H2AC12, H2AC14, H2AC17, H2AC19 and H2AC20) were among the top five downregulated proteins (Fig. 4). The two main impacted pathways were the upregulation of the metal regulatory transcription factor 1 (MTF1)-activated gene expression pathway and the downregulation of the arginine methyltransferases (RMTs) methylate histone arginines pathway (Table 1).

Discussion

The intricate molecular landscape of PDAC contributes to treatment inefficacy and a considerable rise in patient mortality rates [28]. Inadequate early diagnostic and prognostic markers and ineffective current therapeutic options add to the factors that result in poor outcomes. There are still challenges in increasing the efficacy of immunotherapeutic strategies in PDAC. Identifying key targets that could regulate the immune response and their associated underlying mechanisms could help circumvent these [29]. In this study, we found C3 and C5 to be upregulated in early PDAC but reduced in late-stage disease. We further demonstrated that their pharmacological inhibition increased cell proliferation and migration *in vitro*.

This study identified increased levels of complement C3 and C5 in early-stage (resectable) PDAC patients. This increase in levels may suggest an activated innate immune response, which can be pro- or anti-tumourigenic. PDAC cells hijack normal cellular processes to foster tumour growth and proliferation. One possible mechanism is increasing the levels of C3 and C5, leading to the production of C3a and C5a and the subsequent recruitment of immune cells to the tumour site by chemotaxis [30]. This immune response can then aid tumour growth by secreting cytokines such as TNF-α and IL-6, which promote angiogenesis and subsequently supply the growing tumour with nutrients and oxygen required for survival [31]. Furthermore, the production of C3a and C5a can attract immunosuppressors such as TGF-β and VEGF and suppressive myeloid cells to the tumour microenvironment and inhibit the anti-tumour functions of CD4 and CD8 cells [32]. This implies that PDAC may increase C3 and C5 to support tumour growth and facilitate the development of a suppressive tumour microenvironment (TME).

A positive correlation between CRP and complement C5 was observed. One study demonstrated that elevated levels of C5 can induce the production of pro-inflammatory cytokines and chemokines, including TNF-α, IL-1β, and IL-6 [33], which are elevated in PDAC [34]. These cytokines amplify the inflammatory response and activate signalling pathways, such as NF-κB and STAT3, that promote cell proliferation, survival and angiogenesis [6]. Furthermore, CRP binds C5 to activate complement and secrete pro-inflammatory cytokines [35]. The interaction between CRP and C5 may produce Reactive Oxygen Species (ROS) species, which may induce DNA damage through dysregulated mitochondrial protein, as shown in this study when complement is inhibited. C5 and CRP may synergistically collaborate to fuel inflammatory processes that may or may not support tumour growth in PDAC.

Interestingly, C3 and C5 plasma levels were reduced in late- compared to early-stage PDAC. This may suggest an active immune response and activation of the complement pathway in the early stages of cancer [36]. On the other hand, as PDAC progresses, the immune system may become compromised, leading to a decrease in C3 and C5 levels. We showed that inhibiting the complement pathway increases MIA PaCa-2 cells at the G0 phase and induces cell cycle arrest at the S phase by modulating the cell cycle-regulating protein Cyclin D1, which allowed the G1 to S phase transition seen in the increase of cells in the S phase following treatment, representing cancer progression. Studies have shown that, due to their genetic modification to proliferate faster, cancer cells minimise the time in the G0 phase of cell replication [37]. Within the TME, complement proteins can activate key signalling pathways, such as the PI3K/AKT, MAPK/ERK, or NF-κB pathways, involved in diverse cellular processes that promote tumorigenesis [38]. Multiple studies have shown that inhibiting the complement pathway in ovarian and colon cancer and melanoma reduces tumour growth [9,39,40]. However, the role of the com-

necting chromatin and regulating gene expression. Studies have shown that the dysregulation of these molecules may result in aberrant cell cycle progression, genome instability, DNA damage response and transcriptional regulation [42]. It has been suggested that pancreatic cancer cells may downregulate specific chromatin-remodelling proteins essential for DNA repair [28,43,44].

Conclusion

The findings of this study demonstrated that early PDAC exhibits high expression levels of C3 and C5, which decrease as the severity of the tumour increases. Inhibition of the complement pathway was shown *in vitro* to result in a more aggressive phenotype by stimulating cellular growth, proliferation, and migration, indicating the involvement of complement C3 and C5 in tumour progression. Our findings suggest the dysregulation of the complement pathway in PDAC progression may further help in understanding the context-specific role of the complement pathway in carcinogenesis. Future studies are required to investigate the expression of complement proteins in a larger cohort and further unravel the role of the complement pathway in PDAC. However, depending on the context, it seems it could have both pro and anti-tumourigenic roles. Furthermore, additional studies should be conducted using 3D or *in vivo* models, which better represent the TME of PDAC. Lastly, investigations into pathways linked to the regulation of the complement pathway would be beneficial in further elucidating its role in PDAC.

Availability of Data and Materials

The data in this study is available upon request.

Author Contributions

EEN conceptualised the study. ZN, GC, and EEN acquired funding for the project. ZN, PN, and EEN collected data. ZN, PN, JD, JOJ, MS, TNA, GC, and EEN performed data analysis and interpretation. ZN, PN, TNA and EEN wrote the initial draft. All authors contributed to editorial changes in the manuscript. All authors read and approved the final manuscript. All authors have participated sufficiently in the work and agreed to be accountable for all aspects of the work.

Ethics Approval and Consent to Participate

Ethical clearance for this study was obtained from the Human Research Ethics Committee (Medical) of the University of Witwatersrand (M190734 and M140317). Before sample collection, all participating individuals gave written informed consent.

Acknowledgment

The authors acknowledge the clinical staff of the Hepatopancreatobiliary Unit at Chris Hani Baragwanath Hospital, Johannesburg, South Africa. Dr Nnenna Elebo for assistance with the collection of blood samples. Ms Ntombikayise Xelwa for providing support in cell culturing. Ms Karabo Mosiane for assistance with the usage of the flow cytometry instrument.

Funding

The study was funded by the National Research Foundation grant (Grant number: 138367), the Cancer Association of South Africa (CANSA), and the University of the Witwatersrand Faculty Research Committee Individual Grant.

Conflict of Interest

The authors declare no conflict of interest.

Supplementary Material

Supplementary material associated with this article can be found, in the online version, at https://doi.org/10.23812/j.biol.regul.homeost.agents.20243802.94.

References

[1] Halbrook CJ, Lyssiotis CA, Pasca di Magliano M, Maitra A. Pancreatic cancer: Advances and challenges. Cell. 2023; 186: 1729–1754.
[2] Li KY, Yuan JL, Trafton D, Wang JX, Niu N, Yuan CH, *et al*. Pancreatic ductal adenocarcinoma immune microenvironment and immunotherapy prospects. Chronic Diseases and Translational Medicine. 2020; 6: 6–17.
[3] Siegel RL, Miller KD, Wagle NS, Jemal A. Cancer statistics, 2023. CA: A Cancer Journal for Clinicians. 2023; 73: 17–48.
[4] Nsingwane Z, Candy G, Devar J, Omoshoro-Jones J, Smith M, Nweke E. Immunotherapeutic strategies in pancreatic ductal adenocarcinoma (PDAC): current perspectives and future prospects. Molecular Biology Reports. 2020; 47: 6269–6280.
[5] Singh N, Baby D, Rajguru JP, Patil PB, Thakkannavar SS, Pujari VB. Inflammation and cancer. Annals of African Medicine. 2019; 18: 121–126.
[6] Hussain N, Das D, Pramanik A, Pandey MK, Joshi V, Pramanik KC. Targeting the complement system in pancreatic cancer drug resistance: a novel therapeutic approach. Cancer Drug Resistance (Alhambra, Calif.). 2022; 5: 317–327.
[7] Merle NS, Church SE, Fremeaux-Bacchi V, Roumenina LT. Complement System Part I - Molecular Mechanisms of Activation and Regulation. Frontiers in Immunology. 2015; 6: 262.
[8] Afshar-Kharghan V. The role of the complement system in cancer. The Journal of Clinical Investigation. 2017; 127: 780–789.
[9] Ain D, Shaikh T, Manimala S, Ghebrehiwet B. The role of complement in the tumor microenvironment. Faculty Reviews. 2021; 10: 80.
[10] Revel M, Daugan MV, Sautés-Fridman C, Fridman WH, Roumenina LT. Complement System: Promoter or Suppressor

of Cancer Progression? Antibodies (Basel, Switzerland). 2020; 9: 57.

[11] Xiao Z, Yeung CLS, Yam JWP, Mao X. An update on the role of complement in hepatocellular carcinoma. Frontiers in Immunology. 2022; 13: 1007382.

[12] Körber MI, Staribacher A, Ratzenböck I, Steger G, Mader RM. NFκB-Associated Pathways in Progression of Chemoresistance to 5-Fluorouracil in an *In Vitro* Model of Colonic Carcinoma. Anticancer Research. 2016; 36: 1631–1639.

[13] Nweke EE, Naicker P, Aron S, Stoychev S, Devar J, Tabb DL, *et al*. SWATH-MS based proteomic profiling of pancreatic ductal adenocarcinoma tumours reveals the interplay between the extracellular matrix and related intracellular pathways. PLoS ONE. 2020; 15: e0240453.

[14] Tempero MA, Malafa MP, Al-Hawary M, Behrman SW, Benson AB, Cardin DB, *et al*. Pancreatic Adenocarcinoma, Version 2.2021, NCCN Clinical Practice Guidelines in Oncology. Journal of the National Comprehensive Cancer Network: JNCCN. 2021; 19: 439–457.

[15] Kim HS, Gweon TG, Park SH, Kim TH, Kim CW, Chang JH. Incidence and risk of pancreatic cancer in patients with chronic pancreatitis: defining the optimal subgroup for surveillance. Scientific Reports. 2023; 13: 106.

[16] Chomczynski P. A reagent for the single-step simultaneous isolation of RNA, DNA and proteins from cell and tissue samples. BioTechniques. 1993; 15: 532–532–534, 536–537.

[17] Bustin SA, Benes V, Garson JA, Hellemans J, Huggett J, Kubista M, *et al*. The MIQE guidelines: minimum information for publication of quantitative real-time PCR experiments. Clinical Chemistry. 2009; 55: 611–622.

[18] Livak KJ, Schmittgen TD. Analysis of relative gene expression data using real-time quantitative PCR and the 2(-Delta Delta C(T)) Method. Methods (San Diego, Calif.). 2001; 25: 402–408.

[19] Deer EL, González-Hernández J, Coursen JD, Shea JE, Ngatia J, Scaife CL, *et al*. Phenotype and genotype of pancreatic cancer cell lines. Pancreas. 2010; 39: 425–435.

[20] Ligasová A, Vydržalová M, Buriánová R, Brůčková L, Večeřová R, Janošťáková A, *et al*. A New Sensitive Method for the Detection of Mycoplasmas Using Fluorescence Microscopy. Cells. 2019; 8: 1510.

[21] Ricklin D, Lambris JD. Compstatin: a complement inhibitor on its way to clinical application. Advances in Experimental Medicine and Biology. 2008; 632: 273–292.

[22] Kauanova S, Urazbayev A, Vorobjev I. The Frequent Sampling of Wound Scratch Assay Reveals the "Opportunity" Window for Quantitative Evaluation of Cell Motility-Impeding Drugs. Frontiers in Cell and Developmental Biology. 2021; 9: 640972.

[23] Schindelin J, Arganda-Carreras I, Frise E, Kaynig V, Longair M, Pietzsch T, *et al*. Fiji: an open-source platform for biological-image analysis. Nature Methods. 2012; 9: 676–682.

[24] Baichan P, Naicker P, Augustine TN, Smith M, Candy G, Devar J, *et al*. Proteomic analysis identifies dysregulated proteins and associated molecular pathways in a cohort of gallbladder cancer patients of African ancestry. Clinical Proteomics. 2023; 20: 8.

[25] Shannon P, Markiel A, Ozier O, Baliga NS, Wang JT, Ramage D, *et al*. Cytoscape: a software environment for integrated models of biomolecular interaction networks. Genome Research. 2003; 13: 2498–2504.

[26] Doncheva NT, Morris JH, Gorodkin J, Jensen LJ. Cytoscape StringApp: Network Analysis and Visualization of Proteomics Data. Journal of Proteome Research. 2019; 18: 623–632.

[27] Fabregat A, Sidiropoulos K, Viteri G, Forner O, Marin-Garcia P, Arnau V, *et al*. Reactome pathway analysis: a high-performance in-memory approach. BMC Bioinformatics. 2017; 18: 142.

[28] Wang S, Zheng Y, Yang F, Zhu L, Zhu XQ, Wang ZF, *et al*. The molecular biology of pancreatic adenocarcinoma: translational challenges and clinical perspectives. Signal Transduction and Targeted Therapy. 2021; 6: 249.

[29] Zhu YH, Zheng JH, Jia QY, Duan ZH, Yao HF, Yang J, *et al*. Immunosuppression, immune escape, and immunotherapy in pancreatic cancer: focused on the tumor microenvironment. Cellular Oncology (Dordrecht). 2023; 46: 17–48.

[30] Zhou X, Yan Y, Xu M. Immune cell responses in pancreatic cancer and their clinical application. European Journal of Inflammation. 2022; 20: 205873922110443.

[31] Geindreau M, Bruchard M, Vegran F. Role of Cytokines and Chemokines in Angiogenesis in a Tumor Context. Cancers. 2022; 14: 2446.

[32] Thurman JM, Laskowski J, Nemenoff RA. Complement and Cancer-A Dysfunctional Relationship? Antibodies (Basel, Switzerland). 2020; 9: 61.

[33] van den Bosch MHJ, van Lent PLEM, van der Kraan PM. Identifying effector molecules, cells, and cytokines of innate immunity in OA. Osteoarthritis and Cartilage. 2020; 28: 532–543.

[34] Kruger D, Yako YY, Devar J, Lahoud N, Smith M. Inflammatory cytokines and combined biomarker panels in pancreatic ductal adenocarcinoma: Enhancing diagnostic accuracy. PLoS ONE. 2019; 14: e0221169.

[35] Svanberg C, Enocsson H, Govender M, Martinsson K, Potempa LA, Rajab IM, *et al*. Conformational state of C-reactive protein is critical for reducing immune complex-triggered type I interferon response: Implications for pathogenic mechanisms in autoimmune diseases imprinted by type I interferon gene dysregulation. Journal of Autoimmunity. 2023; 135: 102998.

[36] Senent Y, Tavira B, Pio R, Ajona D. The complement system as a regulator of tumor-promoting activities mediated by myeloid-derived suppressor cells. Cancer Letters. 2022; 549: 215900.

[37] Yano S, Miwa S, Mii S, Hiroshima Y, Uehara F, Yamamoto M, *et al*. Invading cancer cells are predominantly in G0/G1 resulting in chemoresistance demonstrated by real-time FUCCI imaging. Cell Cycle (Georgetown, Tex.). 2014; 13: 953–960.

[38] Wang L, Wang L, Zhang H, Lu J, Zhang Z, Wu H, *et al*. AREG mediates the epithelial-mesenchymal transition in pancreatic cancer cells via the EGFR/ERK/NF-κB signalling pathway. Oncology Reports. 2020; 43: 1558–1568.

[39] Surace L, Lysenko V, Fontana AO, Cecconi V, Janssen H, Bicvic A, *et al*. Complement is a central mediator of radiotherapy-induced tumor-specific immunity and clinical response. Immunity. 2015; 42: 767–777.

[40] Zhang R, Liu Q, Li T, Liao Q, Zhao Y. Role of the complement system in the tumor microenvironment. Cancer Cell International. 2019; 19: 300.

[41] Kennedy L, Sandhu JK, Harper ME, Cuperlovic-Culf M. Role of Glutathione in Cancer: From Mechanisms to Therapies. Biomolecules. 2020; 10: 1429.

[42] Mei Q, Huang J, Chen W, Tang J, Xu C, Yu Q, *et al*. Regulation of DNA replication-coupled histone gene expression. Oncotarget. 2017; 8: 95005–95022.

[43] Hasan N, Ahuja N. The Emerging Roles of ATP-Dependent Chromatin Remodeling Complexes in Pancreatic Cancer. Cancers. 2019; 11: 1859.

[44] Sobanski T, Rose M, Suraweera A, O'Byrne K, Richard DJ, Bolderson E. Cell Metabolism and DNA Repair Pathways: Implications for Cancer Therapy. Frontiers in Cell and Developmental Biology. 2021; 9: 633305.